

## Design and Evaluation of a Planar I-Shaped Folded-Patch Antenna for Compact Passive UHF RFID Tags to Cohere on Metal

Yongtao Ma<sup>1, 2, \*</sup>, Hongfei Ning<sup>1, 2</sup>, Weijia Meng<sup>1, 2</sup>, and Chenglong Tian<sup>1, 2</sup>

**Abstract**—A planar I-shaped folded-patch antenna with a footprint of  $21\text{ mm} \times 21\text{ mm} \times 1.6\text{ mm}$  is designed for compact UHF RFID tags to cohere on metal. The antenna consists of three parts: a square ground plane, an I-shaped patch, and a ring resonator. The I-shaped patch is interconnected to the ground plane through a narrow shorting stub, and the microstrip feed line is inserted into the patch to reduce the input impedance of the patch. Extra capacitance and inductance introduced by the ring resonator can lower the tag's resonant frequency down to the expected UHF RFID band. The proposed antenna is manufactured, and there is excellent consistency between simulation and measurement results. The proposed tag antenna achieves a far read distance up to 6.3 m on metal (with 4 W equivalent isotropic radiated power) at resonant frequency of 920 MHz.

### 1. INTRODUCTION

With the development of the Internet of Things technology in various fields, the application scenarios of RFID tags become more diverse. Some of them require the tags to be adhered on objects of different materials, such as glass, wood, and even metal. Among these attached materials, metal, in particular, has the greatest impact on the performance of the antenna. Many designed methods for on-metal tags have been proposed to reduce the influence of the metal. For example, effective solutions are composed of increasing the distance between the tag and the surface of the metal object [1], folding the dipole arm into multiple parts [2], etc. Another way is to introduce an artificial magnetic conductor (AMC) [3, 4] or electromagnetic bandgap (EBG) [5] structures, both of which are capable of isolating the antenna from its backing metal. However, the thickness and cost of the tag will greatly increase while achieving good read performance.

The most common method is to introduce a conductive ground layer under the antenna to form a microstrip patch antenna and a similar multilayer structure [6]. Mo and Qin proposed an open shorted planar patch antenna in 2010 [7], but its size was still large. To solve this problem, Michel and his partners introduced vias [8] to achieve the purpose of miniaturization, but the introduction of vias or pins greatly increases the tag's cost. In 2019, Bong and his team proposed a folded patch antenna to achieve a longer reading range [9, 10].

In this article, an I-shaped folded patch antenna is proposed for adhesion to metal. The dielectric constant of the flexible PET (polyethylene terephthalate) material is 3.3, and the loss tangent is 0.003. Considering the UHF bands of various countries, the performance of the antenna is analyzed and optimized at the resonant frequency with a center frequency of 920 MHz. The proposed tag antenna is very compact. Although it is small, it can achieve a nearly complete matching effect. The antenna is simulated by HFSS, and the equivalent circuit of the antenna is also analyzed. Finally, the proposed antenna is fabricated.

---

Received 22 August 2020, Accepted 14 October 2020, Scheduled 22 October 2020

\* Corresponding author: Yongtao Ma (mayongtao@tju.edu.cn).

<sup>1</sup> School of Microelectronics, Tianjin University, Tianjin 300072, China. <sup>2</sup> China Tianjin Key Laboratory of Imaging and Sensing Microelectronic Technology, Tianjin 300072, China.

## 2. CONFIGURATION AND DESIGN ANALYSIS

### 2.1. Antenna Description

The structure of the proposed tag antenna is shown in Fig. 1(a). The I-shaped patch and ring resonator are not directly connected, but the ring resonator is placed on the back of the I-shaped patch by folding. It is observed that the capacitance and inductance introduced by the ring resonator can reduce the high resonant frequency of the antenna effectively. With reference to Fig. 1(a), the radiator and ground layers are made by etching an aluminum foil ( $9\ \mu\text{m}$ ) which was initially deposited on a single-layered flexible thin PET ( $50\ \mu\text{m}$ ) substrate. For this design, Monza R6 microchip with a read sensitivity of  $-20\ \text{dBm}$  and input impedance of  $11.91 - j118.94\ \Omega$  at  $920\ \text{MHz}$  is used. The top-down view of the completed tag antenna is shown in Fig. 1(b).

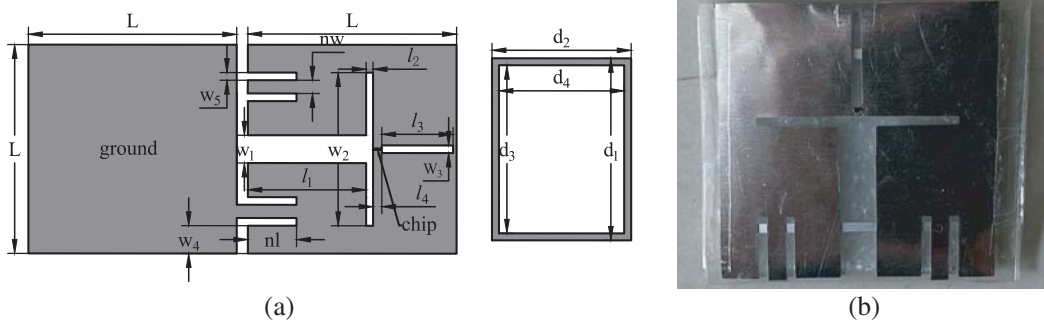


**Figure 1.** (a) Configuration of the proposed tag antenna with design parameters  $L = 21$ ,  $d_1 = 18.31$ ,  $d_2 = 14$ ,  $d_3 = 16.91$ ,  $d_4 = 12.6$ ,  $l_1 = 11.9$ ,  $l_2 = 1.05$ ,  $l_3 = 7.35$ ,  $l_4 = 0.7$ ,  $w_1 = 2.8$ ,  $w_2 = 15.4$ ,  $w_3 = 1.25$ ,  $w_4 = 2.8$ ,  $nl = 5.59$ , and  $nw = 1.33$ . All are in millimeters. (b) Top-down view of the tag.

Now the design procedure of the proposed tag antenna is discussed. The original structure consists of two rectangular patches in both front and back sides. There is a small loop antenna structure on the front patch, and the chip is glued on this structure, as shown in Fig. 2(a). It is found that in this case, the resonant frequency of the tag is greater than  $4.5\ \text{GHz}$ . To shift down the resonance of the tag, the top patch is shorted to the ground plane by a narrow inductive stub. As seen in Fig. 2(a), the tag's resonant frequency is finally  $1.54\ \text{GHz}$ .

To further reduce the resonant frequency, a ring resonator made of concentric high-impedance strip lines is added to the antenna structure. The specific structure is shown in Fig. 2(b). The main innovation is that the loop part can introduce an inductive effect. Though the resonant frequency is tuned to the desired UHF band after introducing the ring resonator, it can only achieve a low antenna resistance

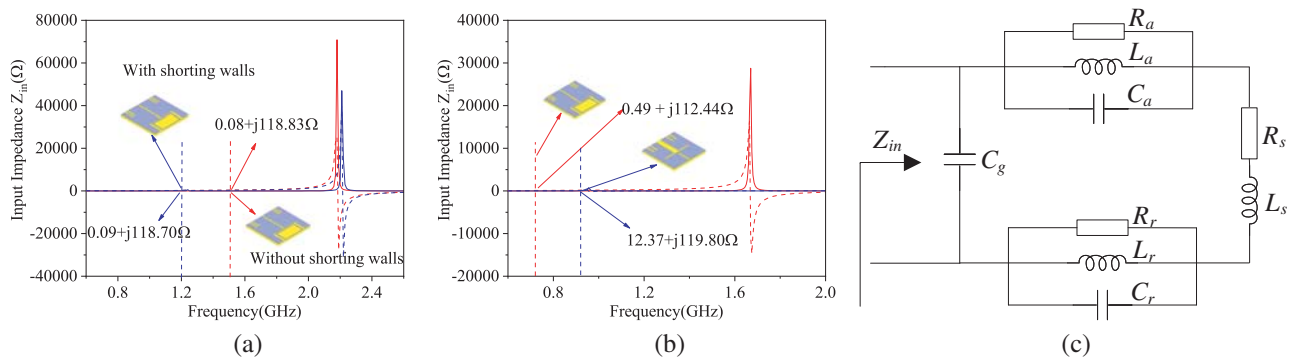


**Figure 2.** (a) Input impedance for cases with and without inductive stubs. (b) Input impedance with and without small loop antenna. (c) Equivalent circuit. ( $C_a = 3.12\ \text{pF}$ ,  $R_a = 21.7\ \text{k}\Omega$ ,  $L_a = 9.366\ \text{nH}$ ,  $C_g = 0.029\ \text{pF}$ ,  $R_s = 0.035\ \Omega$ ,  $L_s = 1.465\ \text{nH}$ ,  $R_r = 13.5\ \text{k}\Omega$ ,  $L_r = 15.118\ \text{nH}$ , and  $C_r = 0.175\ \text{pF}$ ).

$0.49 + j112.44\Omega$ . This is because electrically small antennas generally have very low resistance.

In order to increase the resistance and reduce the inductance, the size of the small loop antenna structure is increased until the small loop antenna is combined with the top radiation patch. The final structure of the tag is modified as shown in Fig. 2(b). It is not easy to adjust multiple parameters at the same time, so the impedance of the antenna is manually adjusted to a range with a relatively small deviation, and then the design parameters is processed by using an optimization program.

## 2.2. Equivalent Circuit Analysis

The equivalent circuit model of the proposed antenna is shown in Fig. 2(c). The parallel resistance  $R_a$ , inductance  $L_a$ , and capacitance  $C_a$  represent the antenna's patch radiator. The patch and ground plane can be viewed as a parallel-plate capacitor, which is called  $C_{pg}$  and  $C_{pr}$  and can be calculated using the following equation:

$$\frac{1}{C_{pg}} = \frac{2h_1}{\varepsilon_{r1}\varepsilon_0 A_1} + \frac{h_2}{\varepsilon_{r1}\varepsilon_0 A_1} + \frac{h_1}{\varepsilon_{r1}\varepsilon_0 A_1}, \quad (1)$$

where the effective area of the patch to the ground plane

$$A_1 = L \times L - 4nl \times sw - l_1 \times w_1 - l_2 \times w_2 - l_3 \times w_3 - l_4 \times g = 0.765 \times 10^{-3} \text{ m}^2,$$

and  $h_1$  and  $h_2$  are the thicknesses of the substrate and the foam, respectively. The parameter  $\varepsilon_0 = 8.854 \times 10^{-12} \text{ F/m}$  is the dielectric constant of free space, and  $\varepsilon_{r1}$  is the permittivity of the PET.

There is a rectangular ring resonator that also forms a parallel-plate capacitor with the antenna's radiation patch in our antenna, which can be represented by  $C_{pg}$ , and it can be estimated using the following equation:

$$C_{pr} = \frac{\varepsilon_{r1}\varepsilon_0 A_2}{2h_1}, \quad (2)$$

where  $A_2 = d_1 d_2 - d_3 d_4 + \left(\frac{d_2 - d_4}{2}\right) \times (w_1 + w_3) = 82.4 \times 10^{-6} \text{ m}^2$  represents the effective area of the ring resonator to the ground plane, and  $C_{pg}$  and  $C_{pr}$  are connected in parallel to form the patch capacitor  $C_a$ . The resistance  $R_a$  can be obtained by the basic calculation formula of  $R = \rho l/S$ , and the calculation method of the inductance  $L_a$  has been proposed in [9].

The series resistance  $R_s$  and inductance  $L_s$  represent the narrow inductive stub. The resistance can be calculated using the following equation:

$$R_s = \left[ \frac{\rho (h_2 + 3h_1 + nl)}{nwh_3} \right] \times K_c (1 - e^{-x}), \quad (3)$$

where  $\rho = 1.72 \times 10^{-8} \Omega \cdot \text{m}$  is the resistivity of copper,  $h_3 = 9 \times 10^{-6} \text{ m}$  the thickness of copper,  $K_c = 2.151$  the current crowding factor,  $x = [2(1 + h_3/nw) \times (\delta/h_3)]$ , and  $\delta = 2.66 \times 10^{-8} \Omega \cdot \text{m}$  is the skin depth of copper. The inductance can be calculated using the following equation:

$$L_s = 2(h_2 + 3h_1 + nl) \left\{ \ln \left[ 2 \frac{h_2 + 3h_1 + nl}{h_3 + nw} \right] + 0.50049 + \frac{h_3 + nw}{3(h_2 + 3h_1 + nl)} \right\}, \quad (4)$$

among them, the unit of the relevant length is centimeters, and the unit of inductance is Naheng (nH).

The capacitance of the gap in which the chip is located is  $C_g$ , and it can be computed using the following equation:

$$C_g = \varepsilon_{r1}\varepsilon_0 l_4 \frac{\left\{ \ln [0.25] + \left(\frac{h_2}{g}\right)^2 + \frac{h_2}{g} \tan^{-1} \left(\frac{2h_2}{g}\right) \right\}}{2\pi} \quad (5)$$

Next, the equivalence of the ring resonator will be discussed, and it can be represent by a resistance  $R_r$ , an inductance  $L_r$ , and a capacitance  $C_r$ . The resistance's value is given in the following equation:

$$R_r = \rho \left\{ \frac{2d_4}{h_3 (d_1 - d_3)/2} + \frac{2d_1}{h_3 (d_2 - d_4)/2} \right\} \quad (6)$$

The calculation method of  $L_r$  is similar to that of  $L_s$ , and the calculation method of the capacitor  $C_r$  is the same as the method of  $C_{pg}$ , as long as the effective area  $A_1$  is replaced by the area of the ring resonator. In summary, the input impedance of the proposed antenna  $Z_{in}$  can be derived as

$$Z_{in} = \frac{Z_{cg}(Z_1 + Z_2 + Z_3)}{Z_{cg} + Z_1 + Z_2 + Z_3}, \quad (7)$$

where  $Z_{cg} = 1/j\omega C_g$ ,  $Z_1 = j\omega R_a L_a / R_a - \omega^2 R_a L_a C_a + j\omega L_a$ ,  $Z_2 = j\omega R_r L_r / R_r - \omega^2 R_r L_r C_r + j\omega L_r$ , and  $Z_3 = (R_s + j\omega L_s)$ . Fig. 3(c) illustrates that the simulations are in line with the equivalent circuit model.

### 3. PARAMETRIC ANALYSIS

First, the effect of changing the dimensions of the inductive stub is studied, and the simulation results are shown in Fig. 3. Increasing or reducing the length or width of the inductive stub will make the antenna become more inductive. It has been confirmed from the calculation that it would also cause  $L_s$  to change. It can be seen from Fig. 3(a) that the resonant frequency of the tag moves 6.34 MHz to the right with 1 mm reduction of  $nl$ . From Fig. 3(b), it is observed that when the value of the  $nw$  becomes lower, the input resistance and reactance of the proposed tag antenna will increase. Fig. 3 shows that  $nw$  and  $nl$  can be used for coarse-tuning of the antenna impedance.

Next, the size of the ring resonator and the interaction of the gap ( $w_3$ ) on the input impedance of the proposed tag antenna are studied. The simulation results are shown in Fig. 4. Changing  $d_2$ ,  $d_1$ , and  $w_3$  causes the resonant frequency to vary at the rates of 1.1, 14.2, and 70 MHz/mm, respectively. The resonant frequency of the tag increases as the size of  $d_1$  and  $w_3$  decreases, causing the proposed tag antenna to become more resistive (increase in tag resistance) and inductive (increase in tag reactance),

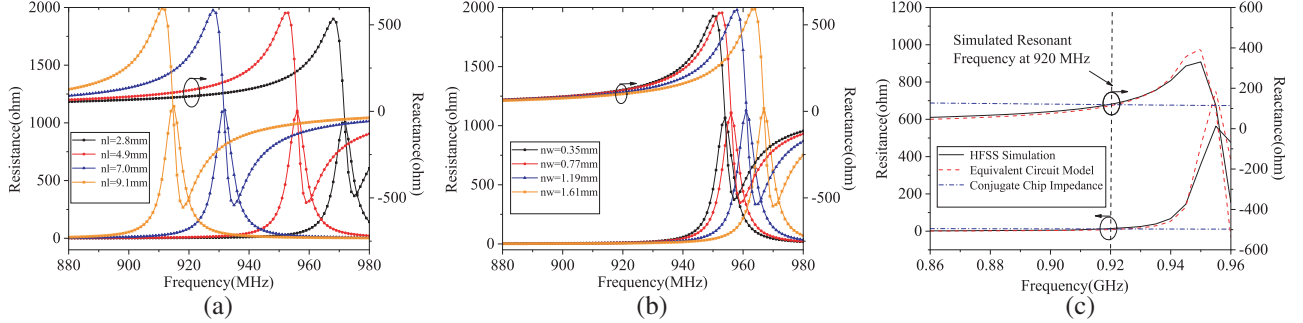


**Figure 3.** Effects of changing the size of the ring resonator and the gap with  $w_3$  on the input impedance. Other parameters remain unchanged.

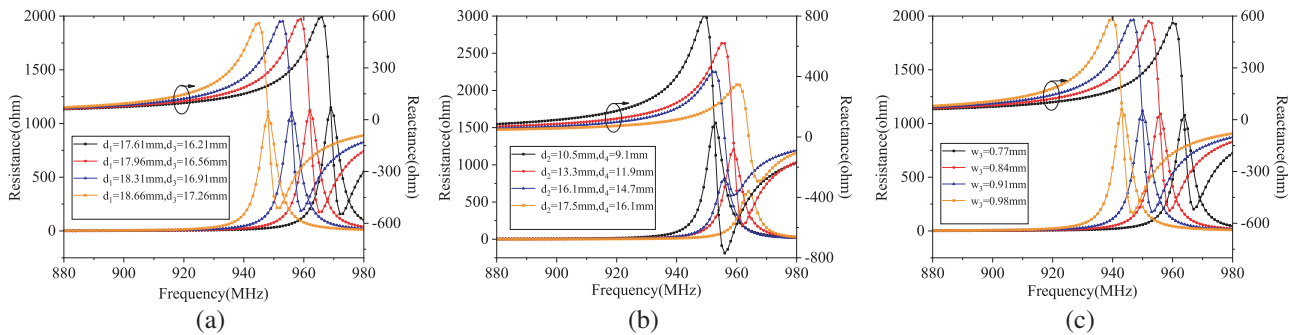


**Figure 4.** Effects of changing the size of the ring resonator and the gap with  $w_3$  on the input impedance. Other parameters remain unchanged.

and it shows that  $d_1$  and  $w_3$  can be used for coarse-tuning of antenna impedance. Besides,  $d_2$  is used to fine-tune the antenna’s input impedance, which is beneficial for adjusting the antenna impedance.

#### 4. REALIZATIONS AND MEASUREMENTS

Figure 5(a) describes the radiation pattern of the tag antenna simulation at the 920 MHz when the main cutting plane of the tag antenna is  $xy$  plane. It can be seen that the maximum gain of the designed antenna is  $-3.5$  dBi. Fig. 5(c) shows the experimental setup in an open environment, where the tag antenna is located in the center of a  $20\text{ cm} \times 20\text{ cm}$  metal plate, and the reader antenna is in the direction of its visual axis. The transmitting and receiving antennas are aligned in parallel, and the tag is moved slowly until the reader cannot read up to the electronic tag, measure the maximum reading distance. The reader antenna uses the laird RFID antenna, and the type is S9028PCR. The reader uses impinj R420. A fixed maximum equivalent isotropic radiated power  $P_r = P_{tx} \cdot G_{tx} = 4\text{ W}$  is used for the measurement, where  $P_{tx}$  is the transmit power of the reader, and  $G_{tx} = 9\text{ dBi}$  is the gain of the reader antenna. Fig. 5(b) shows the tag read distance when the tag antenna is placed at the center of a  $20\text{ cm} \times 20\text{ cm}$  metal plate. It is observed that the maximum read distance of the tag is  $6.3\text{ m}$  at the frequency of  $920\text{ MHz}$ , and we find that the read distance measured at the resonant frequency is slightly lower than the theoretical calculation value. The discrepancies can be caused by experimentation and component tolerances. The deformation of the inlay during the folding process will cause the fluctuation of the effective capacitance and inductance of the antenna.

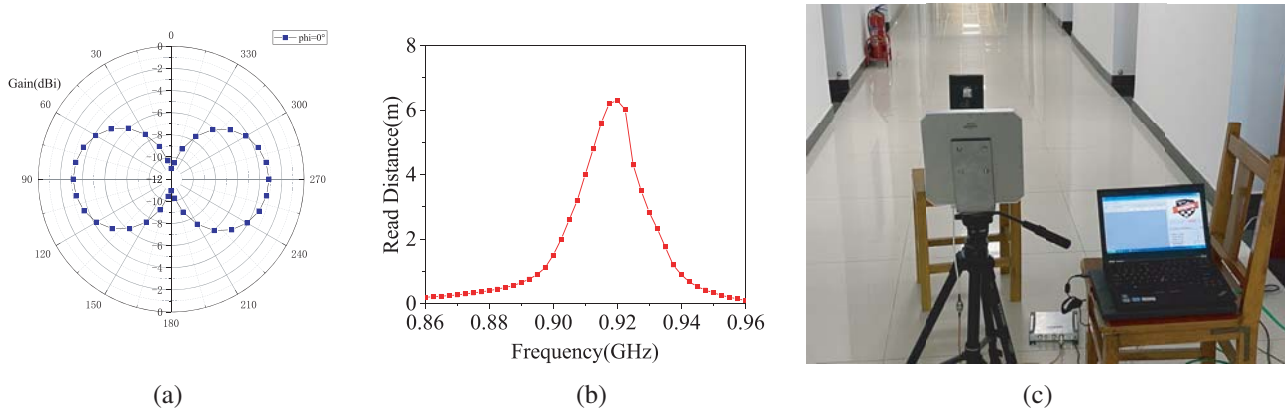


**Figure 5.** (a) Radiation pattern. (b) Read distance. (c) Measure system.

The proposed tag antenna is also compared with some contemporary metal-mountable UHF tags available in the literature, as shown in Table 1. It can be seen that the proposed tag antenna has the best size ratio performance. The antenna proposed in [11] has a similar footprint as this tag, but it is much larger in size than that in this article, and the read distance achieved by it is shorter than ours.

**Table 1.** Comparing the performances of the UHF RFID tags to cohere on metal.

Ref.	Chip Sensitivity (dBm)	Flexibility	Shorting Elements	Tag size (mm) ( $l, w, h$ )	Backing Plate Size (cm)	Power (EIPR)	Max. Read Dist. (m)
[11]	-20	Yes	Stubs	$42 \times 50 \times 1.6$	$20 \times 20$	4 W	5.2
[12]	-17	No	Vias	$45 \times 45 \times 1.27$	$20 \times 20$	4 W	6.8
[13]	-18	Yes	Stubs	$30 \times 30 \times 3$	$20 \times 20$	4 W	7.2
[14]	-20	No	Vias	$55 \times 20 \times 1.6$	$20 \times 20$	4 W	1.8
Here	-20	Yes	Stubs	$21 \times 21 \times 1.6$	$20 \times 20$	4 W	6.3

Although the tag antennas proposed in [12] have a read distance close to ours, their antennas have a larger footprints, which may make them limited in many practical applications. In addition, the antenna requires additional manufacturing processes and introduces parasitic effects. Also, compared with the tags in [13] and [14], the proposed tag has a smaller volume and longer maximum read distance.

## 5. CONCLUSIONS

A planar I-shaped folded-patch antenna is designed for compact UHF RFID tags for on-metal applications. There is a ring resonator to shift down its resonant frequency to the UHF band. Besides, the proposed tag antenna has multiple design parameters, so that it can achieve different levels of coarse and fine tuning to achieve conjugate matching with the chip impedance. It can achieve a maximum read distance of 6.3 m when being tested on a 20 cm  $\times$  20 cm metal plate.

## ACKNOWLEDGMENT

This work is supported by the National Natural Science Foundation of China under Grant 61671318, 61972279.

## REFERENCES

1. Shi, Y., C. Fang, K. Qi, and C.-H. Liang, "A broadband design of UHF fractal RFID tag antenna," *Progress In Electromagnetics Research Letters*, Vol. 58, 45–51, 2016.
2. Guan, M., D. Liang, X. Wang, Y. Wang, and L.-J. Deng, "Magnetic substrate folded dipole antenna for UHF RFID metal tag," *Progress In Electromagnetics Research Letters*, Vol. 47, 25–30, 2014.
3. Ripin, N., E. Lim, F. Bong, and B. Chung, "Miniature folded dipolar patch with embedded AMC for metal mountable tag design," *IEEE Transactions on Antennas and Propagation*, Vol. 68, No. 5, 3525–3533, 2020.
4. Kim, D. and J. Yeo, "Low-profile RFID tag antenna using compact AMC substrate for metallic objects," *IEEE Antennas and Wireless Propagation Letters*, Vol. 7, 718–720, 2008.
5. Li, X., G. Gao, H. Zhu, Q. Li, and N. Zhang, "UHF RFID tag antenna based on the DLS-EBG structure for metallic objects," *IET Microwaves, Antennas Propagation*, Vol. 14, No. 7, 567–572, 2020.
6. Kuo, S. and L. Liao, "An analytic model for impedance calculation of an RFID metal tag," *IEEE Antennas and Wireless Propagation Letters*, Vol. 9, 603–607, 2010.
7. Mo, L. and C. Qin, "Planar UHF RFID tag antenna with open stub feed for metallic objects," *IEEE Transactions on Antennas and Propagation*, Vol. 58, No. 9, 3037–3043, 2010.
8. Michel, A., V. Franchina, P. Nepa, and A. Salvatore, "A UHF RFID tag embeddable in small metal cavities," *IEEE Transactions on Antennas and Propagation*, Vol. 67, No. 2, 1374–1379, 2019.
9. Ng, W., E. Lim, F. Bong, and B. Chung, "E-shaped folded-patch antenna with multiple tuning parameters for on-metal UHF RFID tag," *IEEE Transactions on Antennas and Propagation*, Vol. 67, No. 1, 56–64, 2019.
10. Bong, F., E. Lim, and F. Lo, "Miniaturized dipolar patch antenna with narrow meandered slotline for UHF tag," *IEEE Transactions on Antennas and Propagation*, Vol. 65, No. 9, 4435–4442, 2017.
11. Lee, S., E. Lim, F. Bong, and B. Chung, "Slotted folded patch antenna with double-t-slots for platform-insensitive UHF tag design," *IEEE Transactions on Antennas and Propagation*, Vol. 67, No. 1, 670–675, 2019.
12. Zuffanelli, S., G. Zamora, F. Paredes, P. Aguila, F. Martin, and J. Bonache, "On-metal UHF-RFID passive tags based on complementary split-ring resonators," *IET Microwaves, Antennas Propagation*, Vol. 11, No. 7, 1040–1044, 2017.
13. Bong, F., E. Lim, and F. Lo, "Flexible folded-patch antenna with serrated edges for metal-mountable UHF RFID tag," *IEEE Transactions on Antennas and Propagation*, Vol. 65, No. 2, 873–877, 2017.

14. Zhang, Y. J., D. Wang, and M. S. Tong, "An adjustable quarter-wavelength meandered dipole antenna with slotted ground for metallicity and airily mounted RFID tag," *IEEE Transactions on Antennas and Propagation*, Vol. 65, No. 6, 2890–2898, 2017.